AIAA JOURNAL
Vol. 30, No. 4, April 1992

Semiconductor Laser Doppler Anemometer for Applications in Aerodynamic Research

Franz Durst,* Reiner Müller,† and Amir A. Naqwi‡
University of Erlangen-Nuremberg, Erlangen, Germany

Using a laser diode as the light source and an avalanche photodiode as the detector, an anemometry system has been developed that is particularly suitable to applications in aerodynamic research. This device consumes significantly less power than a conventional laser Doppler anemometer system and may easily be operated with the electrical power available in an airplane during flight. It is also very small in size and may be conveniently transported and mounted at places where space is limited, such as an aircraft wing. The hardware of a semiconductor laser Doppler anemometer unit is described in this paper. The performance of the system is evaluated theoretically as well as experimentally. Measurements in boundary layers are presented to demonstrate that a well-optimized semiconductor laser Doppler anemometer system is as reliable as a conventional system based on a gas laser and a photomultiplier tube.

Nomenclature

b = relative error in signal frequency
f_D = Doppler signal frequency
H_{12} = boundary-layer shape factor
k = wave number of laser light
l = radius of the collimating lens
$R_{c\zeta}$, $R_{c\eta}$ = radii of wave-front curvature along ζ and η axes, respectively
U = freestream velocity of the boundary layer
u, v, w = velocity components along x, y, and z axes, respectively (u = streamwise velocity)
u_c = optical field of the collimated beam
$u_{c\zeta}$, $u_{c\eta}$ = partial fields along ζ and η axes, respectively
w_c = $1/e^2$ half-width of the Gaussian distribution in the collimated optical field
x, y, z = coordinates of the laser Doppler anemometer measuring volume (y = distance from the wall)
x_i, y_i, z_i = coordinates of the individual laser beams
γ = half-width of the Lorentzian distribution at the half-maximum
Δ = boundary-layer thickness
Δ_1 = displacement thickness of the boundary layer
ζ, η = coordinates of the collimated laser beam
θ = half-angle between the beams
λ = wavelength of laser light
ϕ_{ix}, ϕ_{iy} = partial transverse phases of the laser light along x_i and y_i axes, respectively
ϕ_{ixy} = transverse phases of the individual beams

Subscript

i = indices for the two laser beams, = 1 or 2

Introduction

LASER Doppler anemometers (LDA) may be used in test sections of dimensions as small as a few millimeters up to as large as several tens of a meter, provided that optical access is available and the flow is seeded with sufficient scattering particles. The conventional hardware for this instrument includes a gas laser and a photomultiplier tube. These components are expensive, fragile, and large in size. For this reason, the practical applications of LDA have been generally restricted to laboratory conditions. The availability of monomode laser diodes with high coherence lengths in combination with avalanche photodiodes (APD) and pin diodes is promoting the development of a new generation of LDA.[1-4] These systems, based on semiconductor lasers and detectors, consume less power and have the advantages of being small in size and relatively inexpensive. This development promises the use of LDA in many new applications, such as studies of vehicle aerodynamics during road tests or investigations of the wing boundary layers of an airplane during flight. Applications in industrial processes also appear feasible, where such systems may be used as flow monitoring devices. However, previously reported measurements with semiconductor LDA have shown high uncertainties. The variance of the measured data has been large. A drift in the calibration constant has also been noticed. In this study, these effects are investigated theoretically as well as experimentally. Reliable layouts for semiconductor LDA are given and demonstrated to yield precise measurements. Velocity profiles of flat-plate boundary layers are included to demonstrate the quality of measurements.

Estimation of Signal Frequency Errors

The present work shows that relative nonuniformity of fringes is the main source of uncertainty in the measurements taken with a semiconductor LDA system. Earlier studies on this effect have been concerned only with Gaussian laser beams.[5,6] The laser diode beams deviate significantly from a Gaussian beam. Furthermore, the error in signal frequency depends not only on the nonuniformity of fringes but also on the method used for processing the nonuniform signals. This aspect of the problem is not considered in the previous studies. The earlier treatments also lose validity if the wave fronts cannot be represented by a single radius of curvature or if the components of the flowfield transverse to the measuring direction are large. Only recently, a rigorous analysis of the frequency error in dual-beam LDA has been presented.[7] Based on this analysis, the performance of a semiconductor LDA system was estimated. The data of frequency error were also obtained experimentally with a precision device for scanning the fringes. The experimental data have verified the theoretical predictions.

The LDA system under consideration is shown schematically in Fig. 1. The diverging beam of the laser diode is col-

Received March 7, 1990; revision received April 15, 1991; accepted for publication April 29, 1991.

*Fluid Mechanics Laboratory, Professor of Fluid Mechanics, Cauerstrasse 4, 8520.

†Fluid Mechanics Laboratory, Research Assistant; currently, Research Scientist, Porsche Automobile Company, Dept. ETA5, P.O. Box 1140, 7251 Weissach.

‡Fluid Mechanics Laboratory, Research Associate, Cauerstrasse 4, 8520.

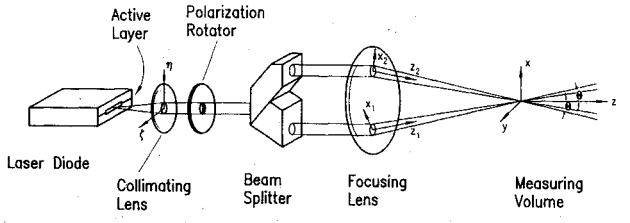

Fig. 1 Focusing optics of a semiconductor LDA: pertinent coordinate systems.

limated using a small focal length lens. If necessary, the axis of polarization of the collimated beam is rotated so that it could be split up into two parallel beams of equal intensity and matched polarization. The front lens serves the usual purpose of bending and focusing the two beams so that they intersect at their focal spots. It is desirable that both of the beams have plane wave fronts in the region of overlap. However, laser diode beams tend to become nonplanar within a short distance from the focal plane, and this contributes to large uncertainties in measurements unless special precautions are taken to suppress this effect. To estimate the magnitude of this effect, an analytical description of the optical field in the measuring volume, as given in Ref. 7, is used.

For the present purpose, a monomode laser diode with emitting power up to 50 mW is considered. As shown in Fig. 1, such a laser has a stripe-type junction that is about 0.1 μm thick and <10 μm wide. Figure 1 also illustrates the laser diode beam as it emerges from the semiconductor junction. Typically, the intensity falls to 50% of the maximum over an angle of 10 deg in the plane of the junction and 30–40 deg normal to it.

For the beam shown in Fig. 1, the electromagnetic field at a point in the cross-sectional plane $\eta\zeta$ may be written as a product of two functions, each dependent on only one of the two transverse coordinates (η or ζ).[8] The optical field distribution along the junction may be considered Gaussian,[9] whereas normal to the junction it may be approximated by Lorentzian distribution.[10] Hence, after collimation, the optical field may be given as follows,

$$u_c(\eta, \zeta) = u_{c\eta}(\eta) u_{c\zeta}(\zeta) \tag{1}$$

where

$$u_{c\zeta}(\zeta) = \exp\left[-\left(\frac{\zeta}{w_c}\right)^2 - i\frac{k}{2}\frac{\zeta^2}{R_{c\zeta}}\right] \tag{2}$$

$$u_{c\eta}(\eta) = \begin{cases} \dfrac{\gamma^2}{\gamma^2 + \eta^2} \exp\left[-i\dfrac{k}{2}\dfrac{\eta^2}{R_{c\eta}}\right] & \text{if } |\eta| \le l \\ 0 & \text{otherwise} \end{cases} \tag{3}$$

In these expressions, the optical fields are expressed as complex functions, such that the arguments of these fields represent the variations in the phase of the waves along η and ζ axes. The values of $R_{c\eta}$ and $R_{c\zeta}$ depend on the spacing between the collimator and the laser diode. Since the beam has a large divergence along η axis, it is truncated at the radius of the lens l. The aberration effects are not included in this model. However, they are discussed qualitatively in interpreting the measured values of frequency error.

Starting with the previous description of the collimated field, the focused field in the measuring volume may be computed by means of the Fresnel formula. Naqwi and Durst[11] have given analytical expressions for the Gaussian distribution of the focused field, whereas a computational procedure is suggested for evaluation of the Lorentzian distribution. Phase behavior of the focused field has a primary significance in the present application. The phases of individual beams may be expressed as follows,

$$-kz_i + \phi_{ixy}, \qquad (i = 1, 2)$$

Figure 1 shows the coordinate systems (x_i, y_i, z_i) for the individual beams. A system of global coordinates (x, y, z) is also shown in this figure. The present investigations are conducted with either ζ or η axis of the collimated field aligned with the y axis, i.e., either the Lorentzian or the Gaussian distribution in the plane of beam intersection. The former case is illustrated in Fig. 1. When the laser diode is rotated through 90 deg, the polarization rotator needs to be adjusted, so that the electric field remains parallel to the y axis. Under this condition, the beam splitter produces two laser beams of equal intensity.

In the special cases just described, the transverse phase of each beam ϕ_{ixy} may be expressed as a sum of the transverse phases (ϕ_{ix} and ϕ_{iy}) of the individual distributions of the optical field along the x and y axes.

In terms of the coordinate systems shown in Fig. 1, the local frequency of an LDA signal may be written as follows,

$$f_D = (1 + b)\frac{2\sin\phi}{\lambda} u \tag{4}$$

where the parameter b represents deviations from the nominal Doppler frequency. It has been derived in Ref. 7 for a generalized nonplanar wave and is given as follows,

$$b = \frac{1}{2k}\left[\left(\frac{\partial\phi_{2x}}{\partial x_2} - \frac{\partial\phi_{1x}}{\partial x_1}\right)\frac{1}{\tan\theta} - \left(\frac{\partial\phi_{2x}}{\partial x_2} + \frac{\partial\phi_{1x}}{\partial x_1}\right)\left(\frac{w}{u}\right) + \frac{\partial(\phi_{2y} - \phi_{1y})}{\partial y}\left(\frac{v}{u}\right)\frac{1}{\sin\theta} + \left(\frac{\partial\phi_{2xy}}{\partial z_2} - \frac{\partial\phi_{1xy}}{\partial z_1}\right)\left(\frac{w}{u}\right)\frac{1}{\tan\theta} - \left(\frac{\partial\phi_{2xy}}{\partial z_2} + \frac{\partial\phi_{1xy}}{\partial z_1}\right)\right] \tag{5}$$

The parameter b depends on the gradients of the transverse phase ϕ_{ixy} of each beam in the plane normal to the main direction of propagation. This is a mere indication of the fact that deviations from the nominal Doppler frequency are caused by nonplanar structure of the beams in the measuring volume, as the preceding gradients vanish for plane waves.

In Eq. (5), the first two terms on the right side have the most significant contribution to the uncertainty in the signal frequency. It may be noticed that the influence of v component of velocity diminishes for a path-length compensated system. Furthermore, the last two terms are less significant because of a generally slow change of the transverse field in the direction of propagation. Hence, it is much more important to eliminate the gradients of the phase (or the wave-front curvature) in the plane of intersection than that normal to it. This readily suggests that it is not necessary to build complicated optics to remove all of the astigmatism from the laser diode beam; accurate measurements can be made with a system having a substantial amount of wave-front curvature normal to the plane of beam intersection. Without any correction for astigmatism, the contribution of this curvature to the frequency error in a typical laser diode LDA is estimated to be $\mathcal{O}(10^{-4})$ or smaller.

Finally, it may be recalled that the frequency given by Eq. (4) is a localized value corresponding to a specific particle location. The time-domain value of the Doppler frequency is estimated by averaging the local frequency along the particle path within the measuring volume. In the case of frequency-domain signal processing, the measured frequency corresponds to the peak of the signal spectrum. The peak frequency is generally different from the average frequency. As a first

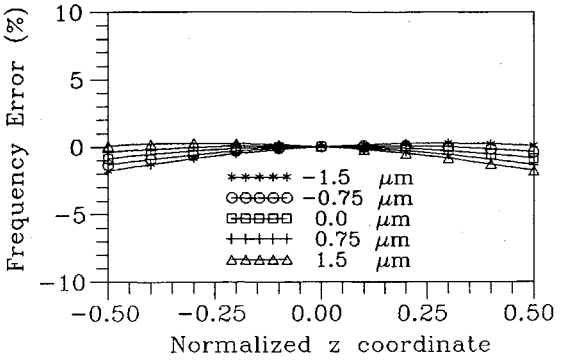

a) Gaussian distribution

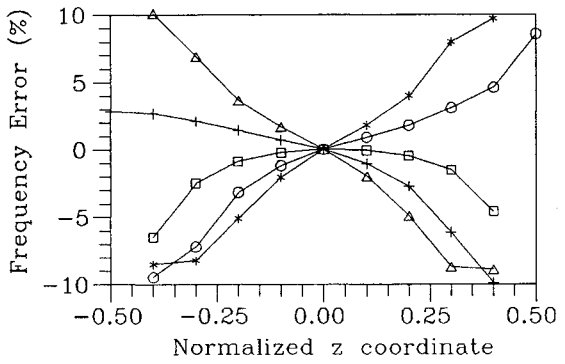

b) Lorentzian distribution: time-domain signal processing

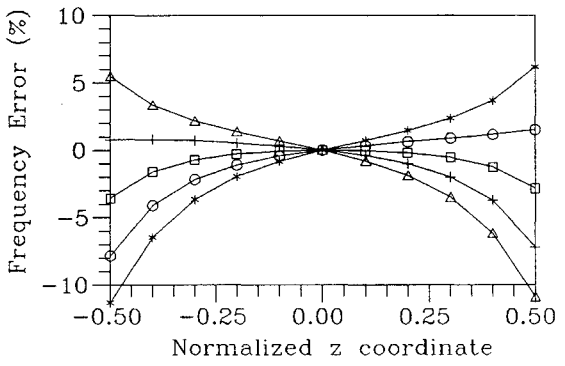

c) Lorentzian distribution: frequency-domain signal processing

Fig. 2 Computed frequency error.

estimate, the peak frequency is assumed to correspond to the saddle point in the central region of the measuring volume. For particles moving parallel to the x axis, the local frequency at $x = 0$ is taken as the peak frequency. Computations have shown that the average frequency coincides with the peak frequency for an aberration-free LDA system using Gaussian distribution in the plane of beam intersection. However, they are appreciably different if the Lorentzian distribution lies in the plane of the beams. The difference becomes larger if the aberration effects are also included.

In Figs. 2, computed values of the parameter b, which represents the relative frequency error, for the present hardware are given as a function of the z coordinate normalized with the length of the measuring volume. In the case of the Gaussian distribution lying in the plane of beam intersection, the measuring volume length is based on $1/e^2$ intensity points. For Lorentzian distribution, the boundaries of the measuring volume are defined as the points where the amplitude of signal fluctuation reduces to 20% of its value at the center. Each curve in these figures corresponds to a particular collimator position. It may be noticed that a substantial deviation from the nominal frequency may be caused merely by micron-size

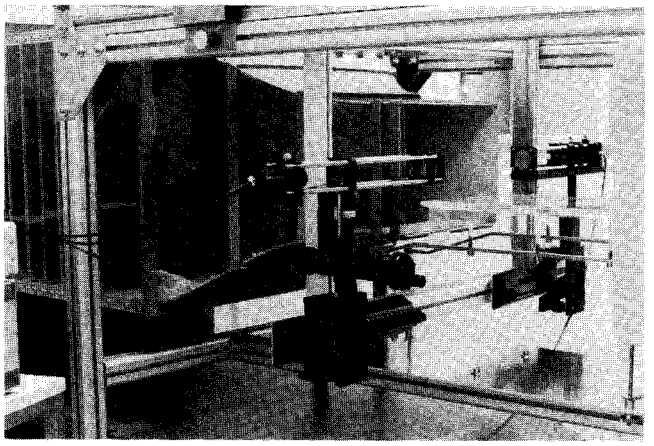

Fig. 3 LDA system mounted on a wind-tunnel test section.

collimator displacements. Results in Fig. 2a pertain to the case of Gaussian distribution and are independent of signal processing method. It is obvious that Gaussian distribution yields smaller frequency errors than Lorentzian distribution. If the Lorentzian distribution must be used in the plane of beam intersection, then it is preferable to perform a spectrum analysis of the signal as it produces better results than time-domain processing.

Measurement of the Frequency Errors

The theoretical estimates of frequency error are compared with the experimental data obtained using an LDA unit, which is shown in Fig. 3. Because of the modular arrangement, the laser diode and the collimator could be replaced to obtain different operating wavelengths and beam cross sections. The front lens could be chosen to obtain the appropriate working distance. This arrangement has been particularly useful for the present phase of evaluation and development.

The overall physical dimensions of the system are 40 × 40 × 230 mm. The pertinent optical data are listed in Table 1. Some of the entries have two values: the first value is valid for evaluation with Lorentzian distribution in the plane of beam intersection, and the second one is applicable when the laser diode has been rotated through 90 deg in order to bring the Gaussian distributions in the plane of the beams.

Scans of the measuring volume for the two cases are shown in Figs. 4 and 5. They exhibit a high modulation depth, indicating that the two beams have about the same intensity and polarization. In Fig. 4, the scans taken at $y = \pm 15$ μm show an intensity distribution that is similar in shape to that at $y = 0$. There is no obvious distortion due to curvature of the wave fronts normal to the plane of beam intersection.

During the experiments, the measuring volume was scanned with a 2-μm pinhole mounted near the edge of a rotating disk of diameter 90 mm. The speed of the motor used to rotate the disk was stabilized within 0.1%. The pinhole was traversed vertically (along the x axis) through the measuring volume. Precision translators were used to position the path of the pinhole in the yz plane. The least count for the readout of

Table 1 Specifications of the laser Doppler anemometer system

Laser diode	Hitachi HL 8314, Hitachi HL 8351
Power	30 mW, 50 mW
Wavelength	830 nm
Beam divergence	
Parallel to junction	10 deg, 9 deg
Perpendicular to junction	27 deg
Focal lengths	
Collimator	6.98 mm, 4.5 mm
Front lens	100 mm
Collimator numerical aperture	0.35, 0.47
Beam spacing	20 mm

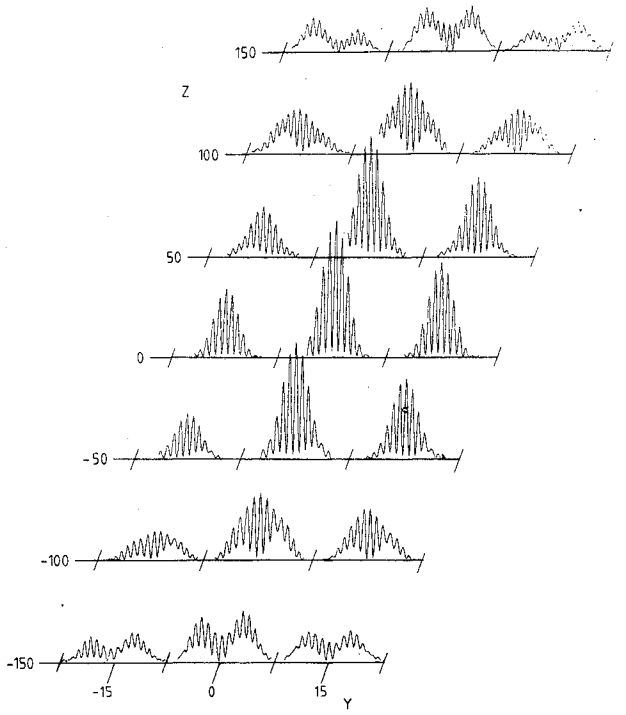

Fig. 4 Intensity distribution in the measuring volume: Lorentzian distribution in the *xz* plane.

the translator position was 0.1 μm, and the specified accuracy of positioning was 0.02 μm.

The light transmitted through the pinhole during each scan was focused onto an APD, which produced an electrical signal simulating a Doppler burst. The measured signal was transmitted to a digital oscilloscope and a counter-type LDA processor. Subsequently, the digitized burst was received by a microcomputer, which performed a fast Fourier transform (FFT) to determine the peak of the spectrum. The reported values of the Doppler frequency were deduced from averages of 20 scans at each measuring location. Typically, the rms value over 20 scans was <0.1% of the mean value.

For the cases of Lorentzian and Gaussian distributions lying in the plane of beam intersection, the counter processor yielded the signal frequency averaged over 4 and 8 cycles, respectively. Since the signals from the Lorentzian distribution have nonuniform periods, a difference of 4% between the frequencies of the first half and the entire signal was necessary for effective validation. For the Gaussian distribution, this tolerance limit was reduced to 1.5%. An average of 1000 scans was taken at each location. The rms value for these measurements was normally smaller than 0.5% of the mean. A significantly higher rms value was observed only near the edges of the measuring volume.

The ambient temperature was not precisely controlled during the measurements. It is estimated that the operating temperature changed by as much as 5°C during the experiments, which corresponds to a displacement of the collimator of about 0.3 μm resulting from thermal expansion of the assembly. This observation should be kept in view in interpreting the results of the measurements.

The values of measured relative error in the signal frequency are presented in Figs. 6. In the case of Lorentzian distribution, see Figs. 6a and 6b, the errors are clearly suppressed with frequency-domain processing. The difference between the counter measurements and the FFT output is more pronounced than predicted. This effect may be attributed to aberration of the collimator, which is not included in the theoretical estimates. It is also due to collimator aberration that measured sensitivity of frequency errors to the collimator position is smaller than that predicted.

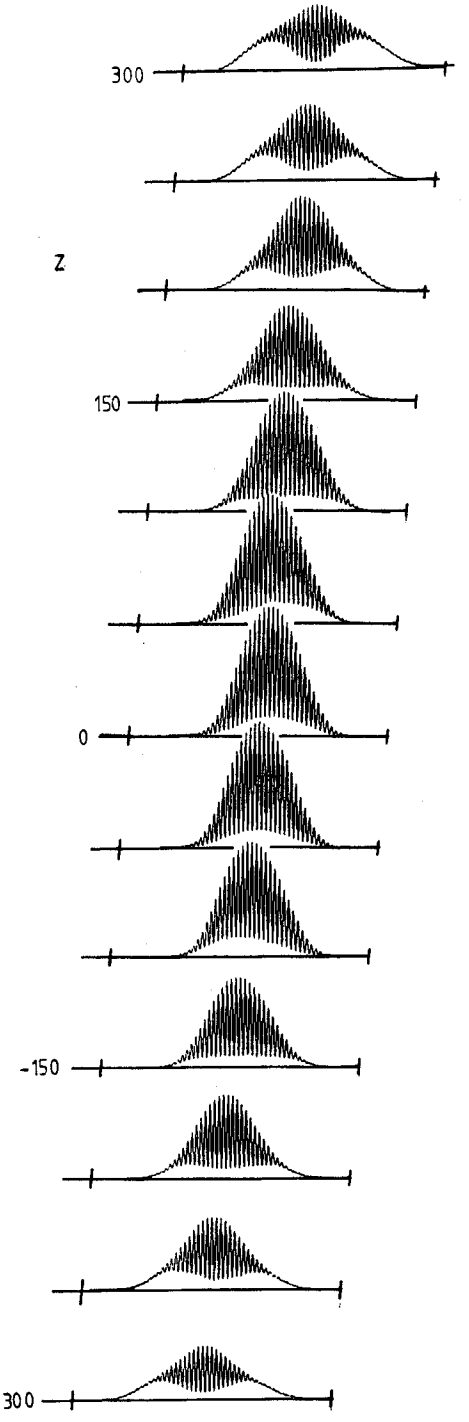

Fig. 5 Intensity distribution in the measuring volume: Gaussian distribution in the *xz* plane.

The Gaussian distribution has a smaller divergence and, hence, the aberration effects are not significant. As shown in Fig. 6c, the measured values of frequency error are small. Also, as predicted, there is no significant difference between the time-domain and frequency-domain signal processing. Since this arrangement involves smaller errors in signal frequency, it was used for the boundary-layer measurements reported in the next section.

Based on the results of theoretical and experimental investigations, some general guidelines may be provided for the design of a semiconductor LDA system. These guidelines are valid for systems with a standard layout as shown in Fig. 1 and that operate with a monomode laser diode of emitting power as large as 50 mW.

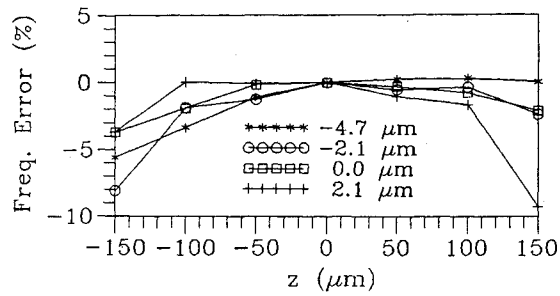

a) Lorentzian distribution: time-domain signal processing

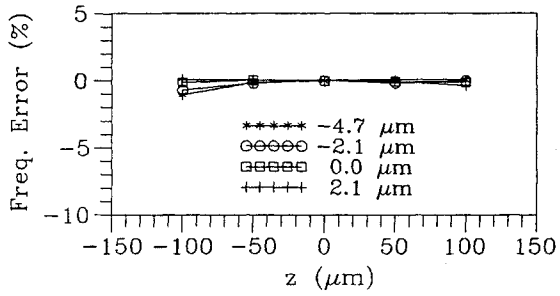

b) Lorentzian distribution: frequency-domain signal processing

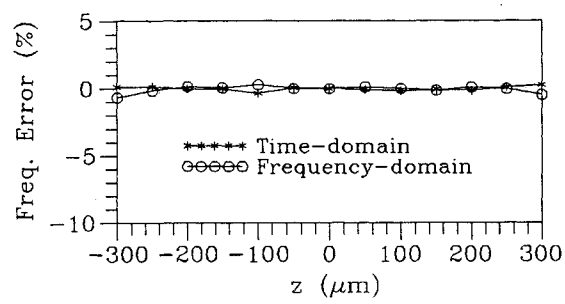

c) Gaussian distribution

Fig. 6 Measured frequency error.

1) For a common application involving turbulence intensities in excess of 1%, it is not necessary to remove ellipticity or astigmatism of the original laser diode beam. It is also not essential to stabilize the wavelength using thermoelectric cooling, provided that the ambient temperature during measurement could be maintained within ±5°C of the temperature at which the LDA system is aligned. The spacing between the laser diode and the collimator must be adjusted with an accuracy of a few microns. A precision scanning device is needed to check the uniformity of fringes during alignment.

2) It is generally preferable to use the Gaussian distribution of the laser diode beam in the plane of beam intersection unless strong focusing is desirable. The use of Gaussian distribution in the xz plane may require a slight misalignment in order to limit the measuring volume along the y axis. Nonetheless, the overall uncertainty in the signal frequency is significantly smaller.

3) For applications involving only a measurement of mean velocity, the system should be calibrated experimentally, as the mean fringe spacing may be larger than $\lambda/2 \sin\theta$.

4) When using the Lorentzian distribution in the xz plane, off-axis collection of scattered light may be needed for measurement of turbulence intensities smaller than 10%.

5) For measuring turbulence intensities smaller than 1%, it would be necessary to stabilize the wavelength of the laser diode. It would also be desirable to avoid thermal misalignment of the collimator. For such applications, thermoelectric cooling should be applied to the entire diode-collimator assembly.

Boundary-Layer Measurements

The present LDA system was built for measurements of boundary-layer profiles on an airplane wing during flight. It is considered appropriate to qualify this system with boundary-layer measurements under laboratory conditions. The experimental setup used for this purpose is described here, and the results of qualification experiments are presented.

The boundary-layer measurements were taken in a Göttingen-type low-speed wind tunnel, which had an open test section 240 mm wide, 170 mm high, and 320 mm long. The test section is shown in Fig. 3. The focusing and receiving optics are located in the front and back side of the test space, respectively. A freestream velocity as high as 20 m/s could be achieved, whereas the freestream turbulence intensity was restricted to 0.5%. A boundary layer was produced by mounting a horizontal flat plate of acrylic glass in the test section. The plate was 220 mm wide and 300 mm long. The leading edge was made smooth, such that its profile conformed to the relevant NACA standard. The LDA unit was mounted on a traversing mechanism, which permitted translation in the streamwise as well as normal directions. A stepping motor was used for precise movement of the forward scattering system in the normal direction. The Doppler signals were transferred to a counter-type signal processor, which was controlled by a microcomputer. To increase the signal rate, the flow was seeded with micron-size smoke particles.

Boundary-layer profiles were measured at a distance of 205 mm from the leading edge of the flat plate and at a freestream velocity of 9 m/s. Starting from the surface, LDA and hot-wire measurements were taken at intervals of 0.15 mm in the normal direction. At larger distances from the wall, the interval between successive measurements was increased to 0.3 mm. In the case of LDA, the first measurement was taken at a point closest to the wall where signals were detectable.

The measured profiles of the mean streamwise velocity and turbulence intensity are presented in Figs. 7a and 7b, respectively. The local velocity has been normalized with the freestream velocity, and the wall distance with the displacement thickness Δ_1. The turbulence intensities are based on

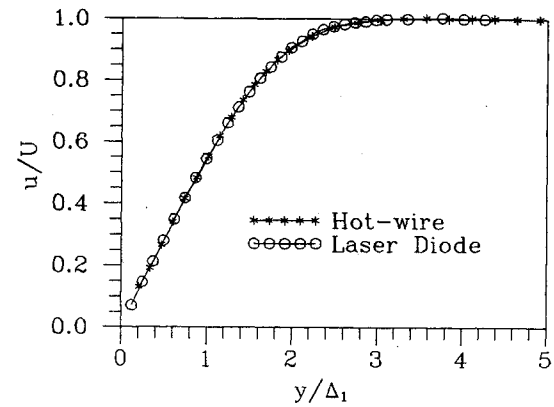

a) Velocity profiles

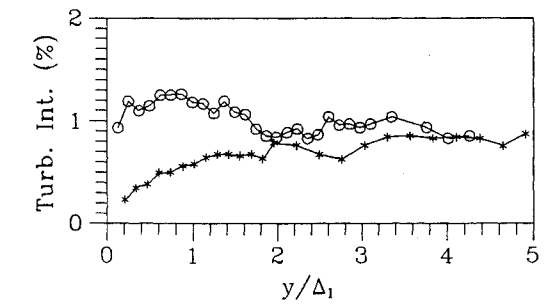

b) Turbulence profiles

Fig. 7 Boundary-layer measurements: laser diode vs hot wire.

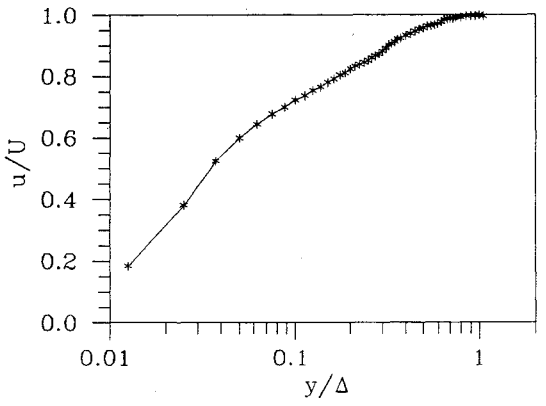

a) Velocity profile

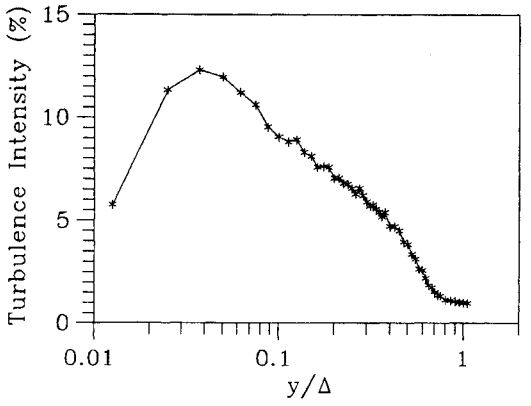

b) Turbulence intensity

Fig. 8 Measurements of the tripped boundary layer.

the freestream velocity. It may be noticed that the profiles of the mean velocity, measured with the hot wire and semiconductor LDA, agree very well. The calculated values of the shape factor H_{12} are 2.60 for both the measurements, indicating that the boundary layer is laminar.

In the freestream, the turbulence intensity measured with the LDA system agrees well with the hot-wire measurements, showing that the turbulence levels as low as 1% may be measured accurately with a well-optimized semiconductor LDA system. However, the value of turbulence intensity measured by the LDA probe increases above the hot-wire measurement with the approach of the wall. This effect may have been caused by a large diameter (about 100 μm) of the LDA measuring volume, which has a limited ability to resolve the large velocity gradients near the wall. If a higher resolution is desirable, then a smaller measuring volume should be employed.

To demonstrate the operation of the LDA system in a turbulent boundary layer, a trip wire was used at a distance of 20 mm from the leading edge. The measurements were taken at a distance of 235 mm from the edge. The profiles of mean velocity and turbulence intensity are presented in Figs. 8. The shape factor of the mean profile is 1.50, which indicates that a complete transition to turbulent layer takes place after tripping. The peak value of turbulence intensity based on the freestream velocity is 12.5%, which is in agreement with the commonly known value of this parameter.

Conclusions

A miniature LDA system based on a semiconductor laser and an avalanche photodiode has been developed for aerodynamic measurements during flight tests. Extensive laboratory tests, guided by a generalized theory of frequency broadening, have led to an optimal design of the LDA system, which is now ready for the intended application.

The present work shows that it is essential to use a precision scanning device for ensuring the uniformity of the fringes in the measuring volume. The collimator of the laser diode beam must be adjusted accurately for obtaining a satisfactorily uniform fringe pattern. It is generally preferable to keep the Gaussian intensity distribution of the diode laser beam in the plane of beam intersection.

A normal application does not require special measures for stabilizing the operating wavelength of the laser diode or conditioning the laser beam. Boundary-layer measurements taken with a simple LDA hardware based on semiconductor devices have yielded satisfactory results. These measurements are comparable in quality to those taken with a gas laser system.

References

[1]Dopheide, D., Taux, G., Reim, G., and Faber, M., "Laser Doppler Anemometry Using Laser Diodes and Solid-State Photodetectors," *Proceedings of the 3rd International Symposium on Laser Anemometry*, Lisbon, 1986.

[2]Brown, R. G. W., Burnett, J. G., and Hackney, N., "A Miniature, Battery Operated Laser Doppler Anemometer," *Proceedings of the 4th International Symposium on Laser Anemometry*, Lisbon, 1988.

[3]Dopheide, D., Faber, M., Reim, G., and Taux, G., "A Portable Frequency Stabilized Laser Diode Backscatter Semiconductor LDA for High Velocity Applications," *Proceedings of the 4th International Symposium on Laser Anemometry*, Lisbon, 1988.

[4]Damp, S., "Battery-Driven Miniature LDA-System with Semiconductor Laser Diode," *Proceedings of the 4th International Symposium on Laser Anemometry*, Lisbon, 1988.

[5]Hanson, S., "Broadening of Measured Frequency Spectrum in a Differential Laser Anemometer due to Interference Plane Gradients," *Journal of Physics D: Applied Physics*, Vol. 6, 1973, pp. 164–171.

[6]Durst, F., and Stevenson, W. H., "Influence of Gaussian Beam Properties on Laser Doppler Signals," *Applied Optics*, Vol. 18, No. 4, 1979, pp. 516–524.

[7]Durst, F., Müller, R., and Naqwi, A., "Measurement Accuracy of Semiconductor LDA Systems," *Experiments in Fluids*, Vol. 10, 1990, pp. 125–137.

[8]Paoli, T. L., "Waveguiding in a Stripe-Geometry Junction Laser," *IEEE Journal of Quantum Electronics*, Vol. QE-13, No. 8, 1977, pp. 662–668.

[9]Cook, D. D., and Nash, F. R., "Gain-Induced Guiding and Astigmatic Output Beam of GaAs Lasers," *Journal of Applied Physics*, Vol. 46, No. 4, 1975, pp. 1660–1672.

[10]Dumke, W. P., "The Angular Beam Divergence in Double-Heterojunction Lasers with Very Thin Active Regions," *IEEE Journal of Quantum Electronics*, Vol. QE-11, No. 7, 1975, pp. 400–402.

[11]Naqwi, A., and Durst, F., "Focusing of Diode Laser Beams: A Simple Mathematical Model," *Applied Optics*, Vol. 29, No. 12, 1990, pp. 1780–1785.